Journal of Photochemistry and Photobiology A: Chemistry 217 (2011) 201–206

Contents lists available at ScienceDirect

Journal of Photochemistry and Photobiology A: Chemistry

journal homepage: www.elsevier.com/locate/jphotochem

Photo-Fenton degradation of resorcinol mediated by catalysts based on iron species supported on polymers

Luis Ferney González-Bahamón[a], Felicien Mazille[b], Luis Norberto Benítez[a,*], César Pulgarín[b,**]

[a] Facultad de Ciencias Naturales y Exactas, Departamento de Química, Universidad del Valle, A.A. 25360 Cali, Colombia
[b] Institut des Sciences et Ingénierie Chimiques, GGEC, Ecole Polytechnique Fédérale de Lausanne, 1015 Lausanne, Switzerland

ARTICLE INFO

Article history:
Received 12 May 2010
Received in revised form 8 September 2010
Accepted 13 October 2010
Available online 21 October 2010

Keywords:
Heterogeneous photo-catalysis
Photo-Fenton
Wastewater treatment
Iron-immobilized polymer

ABSTRACT

Novel Fe supported catalysts were prepared by immobilizing iron species on commercial polyethylene via three different methods: (1) acidic pre-treatment of the polyethylene followed by impregnation in aqueous $Fe(NO_3)_3$, (2) TiO_2 photo-catalytic pre-treatment of the polyethylene followed by forced hydrolysis of $Fe(NO_3)_3$, and (3) direct photo-Fenton attack with concomitant iron deposition on the polyethylene surface. The last method required soft conditions and led to the most photo-active Fe–polyethylene film. With this material, at a non-adjusted initial pH of 5.6 in the presence of H_2O_2, total degradation and 50% of resorcinol mineralization were observed in 40 and 60 min, respectively. Photo-Fenton functionalization/Fe-deposition process was also applied to polypropylene, high-impact polystyrene, and polymethylmethacrylate films. The efficiencies of all the prepared heterogeneous photo-catalysts were similar to that of an homogeneous photo-Fenton system containing the same amount of $Fe^{3+/2+}$ that leached during "heterogeneous" processes. That demonstrated than in our systems mainly homogeneous photo-Fenton reactions were responsible for the resorcinol degradation. The photo-catalytic activity observed for the Fe/polymer was a function of the specific polymer capacity to release the initially deposited iron into the solution.

1. Introduction

Within recent decades, there has been growing concern related to the environmental and the health impacts of pollution caused by toxic/non-biodegradable industrial effluents. Their degradation is necessary to prevent pollutant accumulation in the environment and injury to living organisms. The application of photo-catalytic processes is an attractive alternative for removal of bio-recalcitrant pollutants [1–3]. These technologies are based on the production of highly oxidative radicals such as hydroxyl and hydroperoxyl. Their application in water and air purification [4,5], or disinfection [6,7] has been reported.

Among photo-catalytic processes, homogeneous photo-Fenton oxidation is one efficient route for the degradation of a wide variety of organic compounds in water [8,9]. However, this process has several disadvantages in practical applications: large amounts of chemicals and manpower are required, before treatment, to obtain pH next to 3 in order to prevent ferric oxy-hydroxide precipitation. Besides, catalyst separation can be necessary after treatment if water is to be reused or drunk [10,11].

To overcome the former limitations, some studies have described the immobilization of iron species like aqua-complexes or oxides on different supports including inorganic materials [12–14], fly ash [15], activated carbon [16,17], organic polymeric materials such as membranes (nafion, poly-acrylic acid) [11,18,19], films (polyvinyl fluoride, polyethylene) [20,21] and natural fibers (collagen, cotton) [22]. In general, these materials led to Fenton or photo-Fenton degradation of pollutants in solution, even at a wide range of initial pH values.

Nevertheless, the stability of the immobilized catalyst is a controversial issue because iron dissolution occurs, particularly in the presence of organics with ligands able to chelate/bind iron. This leads to high levels of iron ions in solution (typically 2–14 mg/L) [12,17,23–28]. Hence, many results point to the contribution of homogeneous iron during the degradation of pollutants.

The present study focuses on the deposition of iron species on modified polyethylene (PE) films via three different methods: (1) acidic pre-treatment followed by impregnation in aqueous $Fe(NO_3)_3$, (2) TiO_2 photo-catalytic pre-treatment followed by forced hydrolysis with solution of $Fe(NO_3)_3$, and (3) direct photo-Fenton attack with simultaneous iron cations deposition on the polymer surface. We selected the deposition method that produced

* Corresponding author. Tel.: +57 2 339 32 48; fax: +57 2 339 24 40.
** Corresponding author. Tel.: +41 21 693 4720; fax: +41 21 693 6161.
E-mail addresses: luis.benitez@correounivalle.edu.co (L.N. Benítez), cesar.pulgarin@epfl.ch (C. Pulgarín).

1010-6030/$ – see front matter © 2010 Elsevier B.V. All rights reserved.
doi:10.1016/j.jphotochem.2010.10.009

the most photo-active material and was applied to polypropylene (PP), high-impact polystyrene (PS), and polymethylmethacrylate (PA) films. The photo-catalytic activity of iron-species-coated polymeric films was evaluated for resorcinol (R) degradation. As Fe-ion leaching occurs, the contribution of the homogenous reactions was evaluated during the degradation of the pollutant in solution.

2. Experimental

2.1. Chemicals

Resorcinol, H_2O_2, HNO_3, H_2SO_4, $NaHSO_3$, $Fe(NO_3)_3{\cdot}9H_2O$, $(NH_4)_2Fe(SO_4)_2{\cdot}6H_2O$, $FeSO_4{\cdot}7H_2O$, $NaHCO_3$, were Merck reagents (Buchs, Switzerland) and TiO_2 P-25 commercial powder (anatase to rutile ratio ca. 75:25) was supplied by Degussa AG (Germany) and used as received. Commercial low-density polyethylene, polypropylene, polymethylmethacrylate (Expoplastic, Colombia) and high-impact polystyrene (Estizulia, Venezuela) films had thicknesses of 35 μm. Deionized water (18 MΩ cm and dissolved organic carbon (DOC) < 0.1 mg C/L) obtained by using a Millipore (Milli-Q) was used in all experiments.

2.2. Photo-reactor and photo-catalytic procedure

Photo-degradation experiments were performed with 20 mL of R solution (91 μM), at a non-adjusted initial pH of 5.6, room temperature (28 °C and progressively increased up to ca. 32 °C), and in the presence of H_2O_2 1.2 mM, a H_2O_2 concentration higher than 0.3 mM was guaranteed re-adjusting each 20 min. A H_2O_2 stoichiometric concentration for total R mineralization was used, considering that their excess affects the efficiency of oxidation, because react with the hydroxyl radicals ($HO^\bullet$) for to produce hydroperoxyl radicals ($HO_2^\bullet$) that are less reactive than $HO^\bullet$ (Eq. (1)) [29].

$$HO^\bullet + H_2O_2 \rightarrow HO_2^\bullet + H_2O \quad (1)$$

The residual H_2O_2 was quenched with bisulfite. The experiments were carried out in triplicate under magnetic stirring into the polymeric materials used both as catalyst support and reactor. The radiation incoming to the film was guaranteed by using the minimal pollutant solution layer (<2 mm). Fig. 1 shows the cross-section of photo-reactor system, which consists of a Pyrex® Petri dish supporting the polymer film (Φ = 8 cm). The reactor was subjected to UV light irradiation (Phillips TLD, Nederland) with λ_{max} = 350 nm, and only the upper face of the polymer was exposed to the incoming light (42.8 W/m^2). This type of photo-reactor completely illuminated and without dark compartments as recirculation tubes, was selected to limit errors linked to the parasite Fenton reactions produced on Fe-oxides involuntarily attached to non-illuminated parts of the classical re-circulating systems. Each experimental point of the R degradation kinetics corresponded to one Petri dish, therefore at zero time seven Petri dishes simultaneously were irradiated, and sequentially each was taken for R, DOC and Fe analysis.

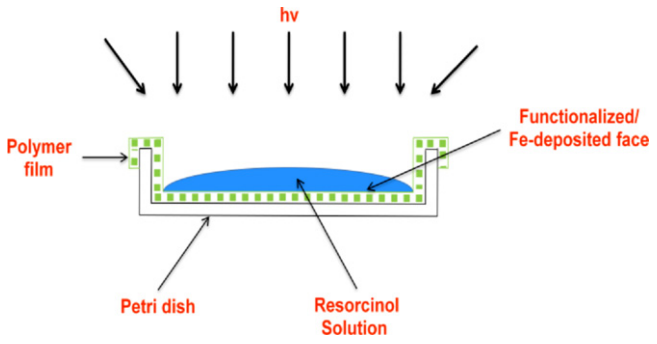

Fig. 1. Cross-section of photo-reactor system with polymeric film.

2.3. Preparation of Fe-immobilized polymeric films

Before modification, the polymer films were washed in ethyl acetate/methanol (1:1) mixture and in Milli-Q water to eliminate surface contaminants. Three different deposition methods were used for the immobilization of iron on PE films in the same reactors described in Fig. 1:

a. Impregnation method: PE film was treated with HNO_3 solution (10%) at room temperature for 18 h. Thereafter, the procedure described by Liu et al. [22] slightly modified, was used for to load iron onto the polymeric film; the material was treated with 30.0 mL of aqueous $Fe(NO_3)_3$ (82.4 mM) at pH ca. 2.0 (adjusted with HNO_3) and the mixture was stirred constantly at 48 °C for 4 h. In order to increase the pH to 3.0, a $NaHCO_3$ solution was slowly added over the course of 2 h, and the reaction proceeded at 48 °C for another 12 h. This material is called PE_{Imp}.
b. TiO_2 photo-catalytic pre-treatment followed by forced hydrolysis: The procedure described by Mazille et al. [20] was slightly modified. The PE film was treated in a dispersed suspension of TiO_2 (0.8 g/L, pH 3.0) for a period of 4 h under UV light (described in Section 2.2) and magnetic stirring. Then the pre-treated PE substrate was immersed in a solution of $Fe(NO_3)_3$ (32.2 mM) and heated to 90 °C during 2 h under stirring. This material is called $PE_{Ti\ F-H}$.
c. Photo-Fenton preparation process: The PE film was immersed in aqueous $FeSO_4$ (0.2 mM) at pH 3.0 for 6 h in the presence of H_2O_2 (10 mM) and under UV light (described in Section 2.2). A decrease up to 50% of iron was observed at the end of the procedure. This material is called PE_{P-F}.

The PP, PA, and PS films had the form shown in Fig. 1 and when treated by method "c", these materials are called PP_{P-F}, PA_{P-F}, and PS_{P-F}, respectively.

All the catalysts obtained were thoroughly washed with deionized water; when the photo-catalyst film showed an iron oxide dusty coat, it was removed with a soft napkin.

2.4. Analyses of photo-treated solutions

Chromatographic analyses of the R solutions were carried out by a Shimadzu LC-2010 chromatograph, equipped with a C-18 analytical column (Agilent Technologies Extend, 5 μm, 250 × 4.6 mm) and mobile phase methanol/Milli-Q water (1:1) at a flow rate of 1 mL/min. R was quantified by UV detector at 274 nm.

The DOC determination was carried out by a Shimadzu 5050 instrument equipped with auto-sampler. The dissolved iron concentration was measured by atomic absorption spectroscopy using a UNICAM AA-939 spectrophotometer with air–acetylene flame. The peroxide in solution was assessed by Merkoquant® paper for concentrations between 0.5 and 25 mg/L.

3. Results and discussion

3.1. Photo-catalytic performance of PE films

Fig. 2 shows the evolution of (i) R, (ii) DOC and (iii) Fe in solution during photo-catalytic experiments using PE_{Imp}, $PE_{Ti\ F-H}$, and PE_{P-F}. Fig. 2(i) shows that R was resistant to photolysis in the presence of H_2O_2 (trace d). R photo-degradation mediated by PE_{Imp} and $PE_{Ti\ F-H}$ films (traces a and b, respectively) in the presence of H_2O_2 was slow, reaching only ca. 20% in 40 min of irradiation and negligible mineralization even after 100 min of irradiation (Fig. 2(ii) traces a

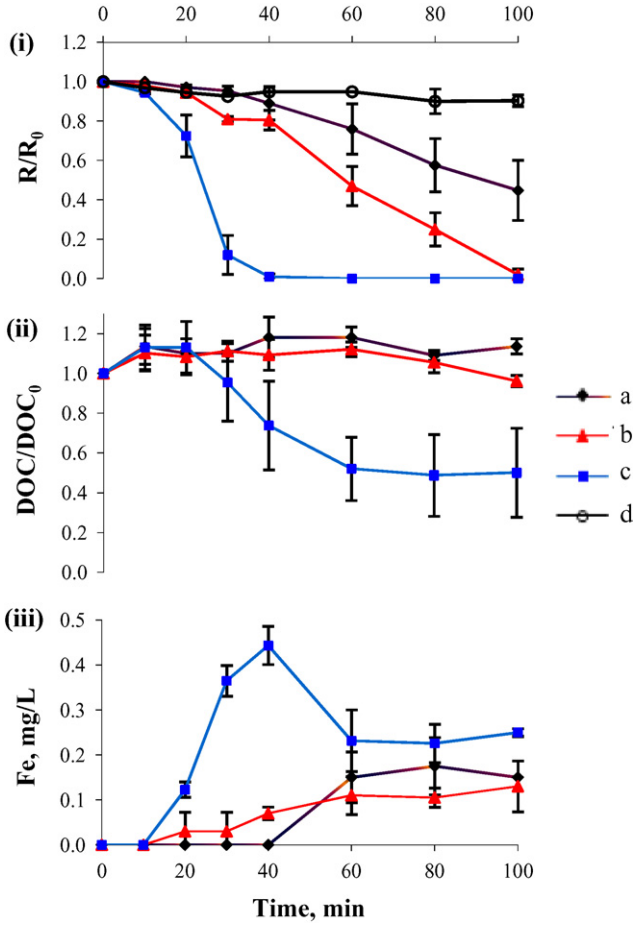

Fig. 2. Normalized concentrations of R (i), DOC (ii), and concentration of iron in solution (iii) during the photo-degradation of R (91 μM) in the presence of H_2O_2 (1.2 mM): (a) PE_{Imp}, (b) $PE_{Ti\ F-H}$, (c) PE_{P-F}, and (d) without catalyst.

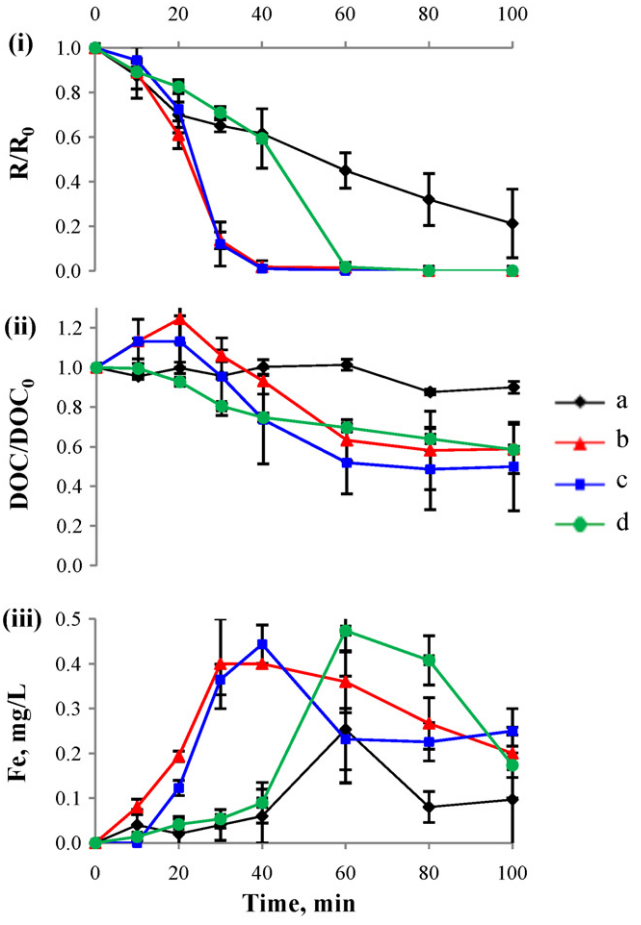

Fig. 3. Normalized concentrations of R (i), DOC (ii), and concentration of iron in solution (iii) during the photo-degradation of R (91 μM) in the presence of H_2O_2 (1.2 mM): (a) PS_{P-F}, (b) PP_{P-F}, (c) PE_{P-F}, and (d) PA_{P-F}.

and b). Low dissolved Fe concentrations (< 0.2 mg/L) were detected (Fig. 2(iii) traces a and b).

In contrast, the PE_{P-F} film showed the highest photo-degradation rates inducing the total disappearance of resorcinol in 40 min (Fig. 2(i) trace c) and 50% of mineralization in 60 min (Fig. 2(ii) trace c), no further mineralization until 100 min was observed. This last result reveals the generation of longer-lived and highly oxidized intermediates. The iron in the solution increases with time up to about 0.4 mg/L within the first 40 min and then decreases to 0.2 mg/L (Fig. 2(iii) trace c). The PE_{P-F} film was clearly the best material able to degrade R, although more iron was leached than with the other films, suggesting that homogeneous catalysis had an important role on the overall process.

3.2. Comparison of different support materials

To establish whether the polymeric support type has some influence on the photo-catalytic activity, four different polymers were subjected to the functionalization/Fe-deposition process by photo-Fenton and comparatively tested for R photo-degradation. Fig. 3 shows the evolution of (i) R, (ii) DOC, and (iii) Fe in solution during photo-catalytic experiments using PE_{P-F}, PP_{P-F}, PA_{P-F}, and PS_{P-F}. During the first 10 min of treatment, the R degradation (Fig. 3(i)) can be associated mainly to the heterogeneous system as the lixiviation of iron ions from the polymers was low (Fig. 3(iii)). Between 10 and 20 min, a different amount of leached iron was observed between PE_{P-F}, PP_{P-F}, and PA_{P-F}, PS_{P-F}. However, the R degradation is not significantly different for all polymers. Fig. 3(ii) shows that DOC increased in the PE_{P-F} and PP_{P-F} systems (curves b and c, respectively) due to parallel corrosion of the Fe/polymer which generates carbonaceous material into the solution. The PP_{P-F} film showed higher self-degradation than the PE_{P-F} film due to its lower chemical stability.

In these initial stages, the Fenton reactions onto polymeric surfaces (≈) lead to the generation of reactive oxygen species, such as $HO^{\bullet}$ and $HO_2^{\bullet}$ radicals (Eqs. (2) and (3)). Surface iron aqua-complexes can be photo-activated to produce more radicals and regenerate the catalyst as shown in Eq. (4). Then, these radicals attack the R molecules in the proximity of the polymer surface (10–300 nm, depending of species) [30,31], leading to aromatic ring opening and the subsequent formation of aliphatic acids as shown in Eq. (5).

$$\approx Fe(III) + H_2O_2 \rightarrow \approx Fe(II) + HO_2^{\bullet} + H^+ \quad (2)$$

$$\approx Fe(II) + H_2O_2 \rightarrow \approx Fe(III) + HO^{\bullet} + HO^- \quad (3)$$

$$\approx Fe(III) + H_2O \xrightarrow{h\nu} \approx Fe(II) + HO^{\bullet} + H^+ \quad (4)$$

$$R + HO_2^{\bullet}/HO^{\bullet} \rightarrow\rightarrow A\text{–}COOH \quad (5)$$

Between 20 and 40 min, increasing R conversion rate is observed with PP_{P-F}, and PE_{P-F} films (Fig. 3(i), curves b and c, respectively) and a concomitant increase in the dissolved Fe concentration is observed (Fig. 3(iii), curves b and c). A similar situation for the PA_{P-F} film between 40 and 60 min is shown in curves d of Fig. 3(i) and (iii). There was a correlation between R degradation, and the iron salts

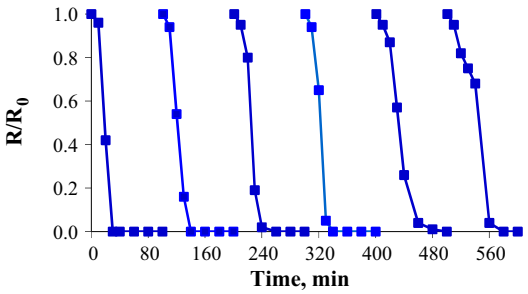

Fig. 4. Repetitive photo-degradation of R (91 μM) at initial pH 5.6 in the presence of H_2O_2 (1.2 mM) and sample PE_{P-F}.

accumulated in the solution by leaching of iron initially fixed on the polymeric films, and consequently the photo-catalytic activity of different polymeric films is mainly linked to their capacity to release soluble Fe forms.

3.3. Long-term activity of the PE_{P-F} catalyst

In order to assess the long-term stability of the photo-catalytic system, experiments were performed with the same PE_{P-F} film. Fig. 4 shows that this material was efficient in degrading R during four successive photo-catalytic cycles, reaching total degradation at reaction time of about 40 min. In two subsequent runs, the degradation rate decreased yielding total elimination of R in 60 min. These results indicate a reduction of ca. 32% in R conversion rate, coinciding with the percentage of iron lost from the film (35%) during the first four cycles. Then, the decay of catalytic activity is associated to leached iron from the catalyst surface.

3.4. Mechanism of functionalization/Fe-deposition

Fig. 5 shows the schematic of the suggested functionalization/Fe-deposition process to originate PE_{P-F}, PP_{P-F}, PA_{P-F}, and PS_{P-F}. The Fenton reagent under light reacts with the polymeric film via HO• radicals leading to the formation of surface CO, COOH, COH, COC, COOC groups and to the elimination of carbonaceous material in the form of short-chain carboxylic acids and CO_2. This hypothesis is supported by experimental evidence because the DOC in the solution was increased (between 1 and 10 mg C/L) at the end of procedure. Using the photo-Fenton process, Fan and co-workers functionalized carbon nanotubes with hydroxyl, carbonyl, and carboxyl groups, which were identified by Fourier Transform Infrared (FTIR) spectral analysis [32]. Due to their nucleophilic character, the groups just mentioned can bind iron ions (Fe^{2+} and Fe^{3+}).

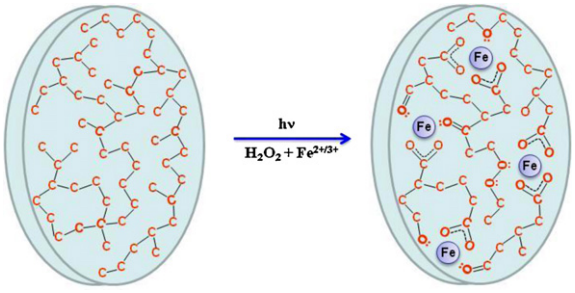

Fig. 5. Schematic diagram for the surface functionalization/Fe-deposition process onto PE through the photo-Fenton method (hydrogen not shown).

3.5. Fe leaching from the PE_{P-F}, PP_{P-F}, PA_{P-F}, and PS_{P-F} films

Unlike photo-catalytic reactors, which use glass containers with and without continuous or semi-continuous water recirculation, the reactors used here allow unambiguous monitoring of iron and guarantee that the solution of R is only in contact with the prepared photo-catalytic material surface. The iron leaching can then arise from its complexation by carboxylic acids generated from R photo-degradation (Eq. (5)), Zazo and co-workers [17] reported the linear correlation between Fe leaching and the amount of accumulated oxalic acid during phenol oxidation by a Fe-immobilized active carbon catalyst in the presence of H_2O_2. Using different catalysts and target pollutants, other groups [23–26,33,34] observed similar iron leakage as shown in Fig. 3(iii) for the polymeric supports. Panias et al. [35] also proposed that the iron dissolution mechanism from oxides involve aliphatic organic acids. Carboxylate groups can form surface Fe(III)–carboxylate complexes (Eq. (6)) and subsequently, undergo charge transfer reactions resulting in the oxidation of the ligands and the reduction of the Fe(III) (see Eq. (7)). Finally, Fe(II) dissolution occurs concomitantly with desorption of the by-products resulting from ligand oxidation (Eq. (8)). For this pathway, the Fe(II) dissolution is very slow, which is enhanced by illumination because the iron–carboxylic acids complexes are photosensitive in the wavelength range used, enhancing ligand-to-metal charge transfer and, consequently, increasing the rate of reaction shown in Eq. (7) [36,37].

$$\equiv Fe(III) + A - COOH \rightarrow \equiv [Fe(III) - (OOC - A)]^- + H^+ \quad (6)$$

$$\equiv [Fe(III) - (OOC - A)]^- \rightarrow \equiv [Fe(II) - (OOC - A)]^- \quad (7)$$

$$\equiv [Fe(II) - (OOC - A)]^- \rightarrow Fe(II) + \text{oxidation products} \quad (8)$$

Dissolved iron concentration reaches a maximum followed by a subsequent decay due to the degradation of $[Fe(II/III)–(OOC–A)]^-$, then Fe-ions are liberated and can return to the functionalized surface of the catalyst or form precipitates.

All polymeric photo-catalysts exhibit a pH decrease from 5.6 to 4.5 during the first 30 min of reaction and remain constant thereafter. This is related to the generation of acidic by-products during the R degradation and to the Fe(II) regeneration by Fe(III) reduction with H_2O_2 as indicated in Eq. (2).

The initial solution pH of 5.6 was not the best for R degradation, since the optimal pH for heterogeneous photo-Fenton processes has been reported to be at pH 3 [12–17,19,23,33,38–41], leading to a high amount of Fe-leaching.

3.6. Contribution of homogeneous photo-Fenton process

To assess the homogeneous contribution due to Fe-leaching into solution during the R photo-degradation by Fe-loaded polymers, experiments were carried out using dissolved Fe(III) with a concentration of Fe equivalent to the Fe-concentration leached from PE_{P-F}, PP_{P-F}, PA_{P-F}, and PS_{P-F} films. Fig. 6 shows that the R degradation and mineralization rates using homogeneous oxidation process (Fe^{3+}/Fe^{2+}, H_2O_2) was similar to those obtained with the studied polymeric "heterogeneous" system. This result suggests that the R oxidation is mainly conducted by HO• radicals coming from photo-Fenton reaction occurring in the solution and probably few coming from the heterogeneous catalyst–solution interface, as discussed in Section 3.2.

Quantification of the heterogeneous photo-Fenton contribution to the overall R conversion and mineralization rates is very difficult. Indeed, depending on the process (homogeneous or heterogeneous) the optical properties of the photo-reactor are modified. Furthermore, the extend of iron leached and consequently its

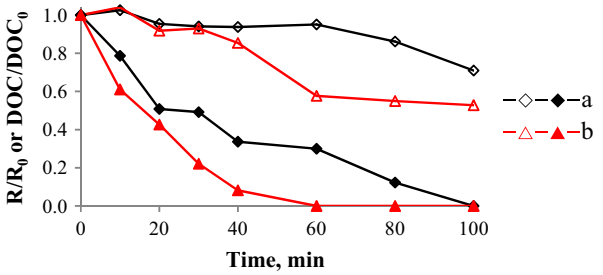

Fig. 6. Normalized concentrations of DOC (open points) and R (full points) during the photo-degradation of R (91 μM) in the presence of H_2O_2 (1.2 mM) with Fe^{3+}: (a) 0.1 and (b) 0.2 mg/L.

concentration in the solution changes as a function of time. Undoubtedly, the hetero/homogeneous process is as efficient as the homogenous one, but the former is advantageous because of the reusability of the photo-catalyst during several runs (see Section 3.3) and the final concentration of iron in the solution is far lower than levels allowed in wastewaters by EEC regulations (2 mg/L) [42].

4. Conclusions

Innovative photo-Fenton catalysts were prepared by immobilizing iron species onto polymer films. Among the preparation methods studied, photo-Fenton functionalization/Fe-deposition led to the most efficient catalysts. This is an innovative method requiring mild preparative conditions: room temperature, aqueous solution, light, and minimal quantities of iron salt.

The best photo-catalytic activities were reached using polyethylene and polypropylene films as supports and the good percentages of resorcinol conversion and mineralization were correlated to iron dissolution.

In the systems studied herein, the main effect exerted by the polymer film on the photo-catalytic activity is the capacity to release iron in solution.

PE_{P-F} is a stable catalyst for the photo-assisted resorcinol decomposition, which can be used in several cycles of degradation with some loss of activity.

Acknowledgements

The authors thank the Colombian Administrative Department of Science, Technology and Innovation (COLCIENCIAS) for its financial support through Grant No. 1106-405-20154, and the UNIVALLE-EPFL cooperation program supported by the biannual agreement between Cooperation@EPFL, and UNIVALLE. Our special thanks to Carolina Borrero, Diego Hoyos and Jhon Angulo for their technical and scientific help and to Juan Kiwi by language corrections.

References

[1] J. Kiwi, C. Pulgarin, P. Peringer, M. Grätzel, Beneficial effects of homogeneous photo-Fenton pretreatment upon the biodegradation of anthraquinone sulfonate in waste water treatment, Appl. Catal. B 3 (1993) 85–99.
[2] M.I. Badawy, F.E.I. Gohary, M.Y. Ghaly, M.E.M. Ali, Enhancement of olive mill wastewater biodegradation by homogeneous and heterogeneous photocatalytic oxidation, J. Hazard. Mater. 169 (2009) 673–679.
[3] P. Ribordy, C. Pulgarin, J. Kiwi, P. Péringer, Electrochemical versus photochemical pretreatment of industrial wastewaters, Water Sci. Technol. 35 (1997) 293–302.
[4] A.M. Ramirez, K. Demeestere, N. De Belie, T. Mäntylä, E. Levänen, Titanium dioxide coated cementitious materials for air purifying purposes: Preparation, characterization and toluene removal potential, Build. Environ. 45 (2010) 832–838.
[5] S. Malato, P. Fernandez-Ibañez, M.I. Maldonado, J. Blanco, W. Gernjak, Decontamination and disinfection of water by solar photo-catalysis: Recent overview and trends, Catal. Today 147 (2009) 1–59.
[6] A. Moncayo-Lasso, J. Sanabria, C. Pulgarin, N. Benítez, Simultaneous *E. coli* inactivation and NOM degradation in river water via photo-Fenton process at natural pH in solar CPC reactor. A new way for enhancing solar disinfection of natural water, Chemosphere 77 (2009) 296–300.
[7] J. Wist, J. Sanabria, C. Dierolf, W. Torres, C. Pulgarin, Evaluation of photocatalytic disinfection of crude water for drinking-water production, J. Photochem. Photobiol. A 147 (2002) 241–246.
[8] P. Saritha, D.S.S. Raj, C. Aparna, Degradative oxidation of 2,4,6-trichlorophenol using advanced oxidation processes – A comparative study, Water Air Soil Pollut. 200 (2009) 169–179.
[9] F. Herrera, C. Pulgarin, V. Nadtochenko, J. Kiwi, Accelerated photo-oxidation of concentrated p-coumaric acid in homogeneous solution. Mechanistic studies, intermediates and precursors formed in the dark, Appl. Catal. B 17 (1998) 141–156.
[10] A.S. Stasinakis, Use of selected advanced oxidation processes (AOPs) for wastewater treatment – A mini review, Global NEST J. 10 (2008) 376–385.
[11] S. Parra, L. Henao, E. Mielczarski, J. Mielczarski, P. Albers, E. Suvorova, J. Guindet, J. Kiwi, Synthesis, testing, and characterization of a novel nafion membrane with superior performance in photo-assisted immobilized Fenton catalysis, Langmuir 20 (2004) 5621–5629.
[12] C. Pulgarin, P. Peringer, P. Albers, J. Kiwi, Effect of Fe-ZSM-5 zeolite on the photochemical and biochemical degradation of 4-nitrophenol, J. Mol. Catal. A: Chem. 95 (1995) 61–74.
[13] H. Xu, M. Prasad, Y. Liu, Schorl: A novel catalyst in mineral-catalyzed Fenton-like system for dyeing wastewater discoloration, J. Hazard. Mater. 165 (2009) 1186–1192.
[14] J. Chen, L. Zhu, Catalytic degradation of Orange II by UV-Fenton with hydroxyl-Fe-pillared bentonite in water, Chemosphere 65 (2006) 1249–1255.
[15] Y.L. Song, J.T. Li, Degradation of C.I. Direct Black 168 from aqueous solution by fly ash/H_2O_2 combining ultrasound, Ultrason. Sonochem. 16 (2009) 440–444.
[16] J.H. Ramirez, F.J. Maldonado-Hodar, A.F. Perez-Cadenas, C. Moreno-Castilla, C.A. Costa, L.M. Madeira, Azo-dye Orange II degradation by heterogeneous Fenton-like reaction using carbon–Fe catalysts, Appl. Catal. B 75 (2007) 312–323.
[17] J.A. Zazo, J.A. Casas, A.F. Mohedano, J.J. Rodríguez, Catalytic wet peroxide oxidation of phenol with a Fe/active carbon catalyst, Appl. Catal. B 65 (2006) 261–268.
[18] Y.C. Li, L.G. Bachas, D. Bhattacharyya, Selected chloro-organic detoxifications by polychelate (poly (acrylic acid)) and citrate-based Fenton reaction at neutral pH environment, Ind. Eng. Chem. Res. 46 (2007) 7984–7992.
[19] J. Fernandez, V. Nadtochenko, O. Enea, A. Bozzi, T. Yuranova, J. Kiwi, Testing and performance of immobilized Fenton photoreactions via membranes, mats and modified copolymers, Int. J. Photoenergy 5 (2003) 107–113.
[20] F. Mazille, T. Schoettl, C. Pulgarin, Synergistic effect of TiO_2 and iron oxide supported on fluorocarbon films. Part 1. Effect of preparation parameters on photo-catalytic degradation of organic pollutant at neutral pH, Appl. Catal. B 89 (2009) 635–644.
[21] M.R. Dhananjeyan, E. Mielczarski, K.R. Thampi, Ph. Buffat, M. Bensimon, A. Kulik, J. Mielczarski, J. Kiwi, Photo-dynamics and surface characterization of TiO_2 and Fe_2O_3 photo-catalysts immobilized on modified polyethylene films, J. Phys. Chem. B 105 (2001) 12046–12055.
[22] X. Liu, R. Tang, Q. He, X. Liao, B. Shi, Fe(III) immobilized collagen fiber: A renewable heterogeneous catalyst for the photo-assisted decomposition of Orange II, Ind. Eng. Chem. Res. 48 (2009) 1458–1463.
[23] A. Bozzi, T. Yuranova, J. Mielczarski, A. Lopez, J. Kiwi, Abatement of oxalates catalyzed by Fe–silica structured surfaces via cyclic carboxylate intermediates in photo-Fenton reactions, Chem. Commun. (2002) 2202–2203.
[24] J. Feng, X. Hu, P.L. Yue, S. Qiao, Photo-Fenton degradation of high concentration Orange II (2 mM) using catalysts containing Fe: A comparative study, Sep. Purif. Technol. 67 (2009) 213–217.
[25] J. Feng, X. Hu, P.L. Yue, H.Y. Zhu, G.Q. Lu, Degradation of azo-dye Orange II by a photo-assisted fenton reaction using a novel composite of iron oxide and silicate nanoparticles as a catalyst, Ind. Eng. Chem. Res. 42 (2003) 2058–2066.
[26] C.P. Huang, Y.H. Huang, Application of an active immobilized iron oxide with catalytic H_2O_2 for the mineralization of phenol in a batch photo-fluidized bed reactor, Appl. Catal. A 357 (2009) 135–141.
[27] W. Najjar, S. Azabou, S. Sayadi, A. Ghorbel, Screening of Fe–BEA catalysts for wet hydrogen peroxide oxidation of crude olive mill wastewater under mild conditions, Appl. Catal. B 88 (2009) 299–304.
[28] C.P. Huang, Y.H. Huang, Comparison of catalytic decomposition of hydrogen peroxide and catalytic degradation of phenol by immobilized iron oxides, Appl. Catal. A 346 (2008) 140–148.
[29] G.V. Buxton, C. Greenstock, W.P. Hellmann, A.B. Ross, Critical review of rate constants for reactions of hydrated electrons, hydrogen atoms and hydroxyl radicals (•OH/•O⁻) in aqueous solutions, J. Phys. Chem. Ref. Data 17 (1988) 513–886.
[30] R. Roots, S. Okada, Estimation of life times and diffusion distances of radicals involved in X-ray-induced DNA strand breaks or killing of mammalian cells, Radiat. Res. 64 (1975) 306–320.
[31] T. Yuranova, O. Enea, E. Mielczarski, J. Mielczarski, P. Albers, J. Kiwi, Fenton immobilized photo-assisted catalysis through a Fe/C structured fabric, Appl. Catal. B 49 (2004) 39–50.
[32] C.L. Fan, W. Li, X. Li, S. Zhao, L. Zhang, Y.J. Mo, R.M. Cheng, Efficient photo-assisted Fenton oxidation treatment of multi-walled carbon nanotubes, Chin. Sci. Bull. 52 (2007) 2054–2062.
[33] M. Bobu, A. Yediler, I. Siminiceanu, S. Schulte-Hostede, Degradation studies of ciprofloxacin on a pillared iron catalyst, Appl. Catal. B 83 (2008) 15–23.

[34] F. Mazille, A. Lopez, C. Pulgarin, Synergistic effect of TiO_2 and iron oxide supported on fluorocarbon films. Part 2. Long-term stability and influence of reaction parameters on photo-activated degradation of pollutants, Appl. Catal. B 90 (2009) 321–329.
[35] D. Panias, M. Taxiarchou, I. Paspaliaris, A. Kontopoulos, Mechanisms of dissolution of iron oxides in aqueous oxalic acid solutions, Hydrometallurgy 42 (1996) 257–265.
[36] T.D. Waite, F.M.M. Morel, Photoreductive dissolution of colloidal iron oxide: Effect of citrate, J. Colloid Interface Sci. 102 (1984) 121–137.
[37] P. Borer, S.J. Hug, B. Sulzberger, S.M. Kraemer, R. Kretzschmar, Photolysis of citrate on the surface of lepidocrocite: An in situ attenuated total reflection infrared spectroscopy study, J. Phys. Chem. C 111 (2007) 10560–10569.
[38] B. Iurascu, I. Siminiceanu, D. Vione, M.A. Vicente, A. Gil, Phenol degradation in water through a heterogeneous photo-Fenton process catalyzed by Fe-treated laponite, Water Res. 43 (2009) 1313–1322.
[39] A. Bozzi, T. Yuranova, J. Mielczarski, J. Kiwi, Evidence for immobilized photo-Fenton degradation of organic compounds on structured silica surfaces involving Fe recycling, New J. Chem. 28 (2004) 519–526.
[40] M. Tekbas, H.C. Yatmaz, N. Bektas, Heterogeneous photo-Fenton oxidation of reactive azo dye solutions using iron exchanged zeolite as a catalyst, Micropor. Mesopor. Mater. 115 (2008) 594–602.
[41] I. Muthuvel, M. Swaminathan, Highly solar active Fe(III) immobilised alumina for the degradation of Acid Violet 7, Sol. Energy Mater. Sol. Cells 92 (2008) 857–863.
[42] EEC List of Council Directives 76/4647, European Economic Community, Brussels, 1976.